Available online at www.sciencedirect.com
ScienceDirect
International Journal of Heat and Mass Transfer 51 (2008) 2824–2833
International Journal of HEAT and MASS TRANSFER
www.elsevier.com/locate/ijhmt

Heat transfer analysis of blast furnace stave

Wu Lijun [a,*], Xu Xun [a], Zhou Weiguo [a], Su Yunlong [b], Li Xiaojing [b]

[a] Department of Thermal Engineering, School of Mechanical Engineering, Tong Ji University, Shanghai 200092, People's Republic of China
[b] Technical Center of Maanshan Iron and Steel Co. Ltd., Maanshan 243000, People's Republic of China

Received 20 October 2006; received in revised form 13 June 2007
Available online 26 November 2007

Abstract

The three-dimensional mathematical model of temperature and thermal stress field of the blast furnace stave is built. The radiation heat transmitted from solid materials (coke and ore) to inner surface of the stave, which has been neglected by other studies, is taken into account. The cast steel stave is studied and the finite element method is used to perform the computational analysis with soft ANSYS. Numerical calculations show very good agreement with the results of experiment. Heat transfer analysis is made of the effect of the cooling water velocity and temperature, the cooling channel inter-distance and diameter, the lining material, the cooling water scale, the coating layer on the external surface of the cooling water pipe as well as the gas clearance on the maximum temperature and thermal stress of the stave hot surface. It is found that reducing the water temperature and increasing the water velocity would be uneconomical. The heat transfer and hence the maximum temperature and thermal stress in the stave can be controlled by properly adjusting operating conditions of the blast furnace, such as the gas flow, cooling channel inter-distance and diameter, lining material, coating layer and gas clearance.

Keywords: Blast furnace; Cooling stave; Heat transfer analysis

1. Introduction

The blast furnace is the equipment which produces molten iron, shown in Fig. 1. The cooling stave is the heat transfer fixture in blast furnace, shown in Fig. 2. Damaged cooling staves are one of the most important reasons that lead to a major overhaul or medium repair of a blast furnace. Therefore, cooling stave life is the key parameter for prolonging campaign life of a blast furnace [1–9]. As ductile cast iron cooling stave cannot meet the need of campaign life well, and the capital cost of a copper stave is too high, there has been a lot of attention for steel cooling stave with high specific elongation, tensile strength, melting temperature and thermal conductivity.

There are many mathematical models describing the heat transfer process of the cooling stave. Steiger [1] developed the heat transfer model to predict the temperature field of copper cooling plate and lining. Wang et al. [2] simulated a three-dimensional heat transfer model to describe the temperature field in the wall of the lower stack region of a blast furnace. Some researchers [3–11] in China have done some numerical simulations to calculate the temperature field of the cooling stave. However, these models apply only to copper or cast iron cooling staves, not to steel cooling staves. Besides, only the temperature field has been considered in these models while the thermal stress field is not calculated. Therefore, these calculation results are unlikely to satisfactorily describe the damage of cooling stave which is mainly caused by thermal stress changes within the cooling stave.

This paper describes a three-dimensional mathematical model of temperature and thermal stress fields for blast furnace steel cooling stave and lining. The effect of the different kinds of parameters on maximum temperature and thermal stress of the stave hot surface has been considered.

* Corresponding author. Tel.: +86 21 6598 1159; fax: +86 21 6598 0273.
E-mail address: ljwu@mail.tongji.edu.cn (L. Wu).

0017-9310/$ - see front matter © 2007 Elsevier Ltd. All rights reserved.
doi:10.1016/j.ijheatmasstransfer.2007.09.030

Nomenclature

c	constant
C_0	Planck constant, 5.67×10^{-8}, W/(m^2 K^4)
c_p	specific heat capacity of cooling water, kJ/(kg K)
d_0	external diameter of the steel pipe, mm
d_1	inner diameter of the steel pipe, mm
E	Young's modulus, Pa
h_k	overall coefficient of heat convection between furnace shell and atmosphere, W/(m^2 °C)
h_{k1}	coefficient of natural heat convection between furnace shell and atmosphere, W/(m^2 °C)
h_{k2}	coefficient of radiative heat transfer from furnace shell to atmosphere, W/(m^2 °C)
h_{wb}	overall coefficient of heat convection between cooling water and stave, W/(m^2 °C)
h_z	overall convection coefficient between high temperature gas flow and solid materials and slag skull, W/(m^2 °C)
l	characteristic length, m
n	constant
R	total heat resistance between cooling water and stave body, (m^2 °C)/W
R_1	convection heat resistance between cooling water and inner surface of steel pipe, (m^2 °C)/W
R_2	conductive resistance of cooling water scale on the inner surface of cooling water pipes, (m^2 °C)/W
R_3	conductive resistance of the steel pipe wall, (m^2 °C)/W
R_4	coating layer on the outer surface of the cooling water pipe, (m^2 °C)/W
R_5	heat resistance of the gas clearance between the cooling water pipe and stave body, (m^2 °C)/W
t	material temperature, °C
t_2, t_c	temperature of the surface of stave body close to the coating layer and of the coating layer surface, °C
T	temperature, °C
T_a	atmospheric temperature, °C
T_2, T_c	absolute temperature correspond to t_2, t_c, K
T_g	gas flow temperature, °C
T_k	temperature of furnace shell, °C
T_{wa}	cooling water temperature, °C
T_{wb}	cooling water pipe ektexine temperature, °C
T_z	slag skull temperature, °C
v	velocity of cooling water, m/s

Greek symbols

α_w	coefficient of heat convection between cooling water and steel pipe, W/(m^2 °C)
λ	thermal conductivity coefficient of material, W/(m °C)
λ_{air}	thermal conductivity coefficient of atmosphere, W/(m °C)
λ_d	thermal conductivity coefficient of water scale, W/(m °C)
λ_c	thermal conductivity coefficient of coating layer, W/(m °C)
λ_e	equivalent thermal conductivity of the gas clearance, W/(m °C)
λ_g	the gas thermal conductivity, W/(m °C)
λ_p	thermal conductivity coefficient of steel pipe, W/(m °C)
λ_w	thermal conductivity coefficient of cooling water, W/(m °C)
ε	emissivity of furnace shell
ε_2	emissivity of stave body
ε_c	emissivity of coating layer
ρ	cooling water density, kg/m^3
υ	kinetic viscosity of cooling water, m^2/s
σ_d	water scale thickness, mm
δ_c	thickness of coating layer on the outer surface of the cooling water pipe, mm
δ_g	thickness of the gas clearance layer,mm
$\sigma_x, \sigma_y, \sigma_z$	respectively x, y, z axial stress, Pa
Θ	bulk force, Pa
$\tau_{xy}, \tau_{yz}, \tau_{zx}$	shear strains, Pa
μ	Poisson's ratio
α_t	coefficient of linear thermal expansion, °C^{-1}

Non-dimensional parameters

Re	the Reynolds number
Nu	the Nusselt number
Pr	the Prandtl number
Gr	the Grash number

2. Model of temperature and thermal stress fields of cooling stave

2.1. Model of temperature field of cooling stave

The cooler apparatus is among slag skull, lining, filling material and furnace shell. A three-dimensional schematic of model is shown in Fig. 3.

In this paper, the heat transfer of the cooling stave and lining is modeled under the steady state conductive heat transfer process. The three-dimensional heat transfer equation can thus be described as follows:

$$\frac{\partial}{\partial x_i}\left(\lambda(T)\frac{\partial T}{\partial x_i}\right) = 0, \quad i = 1, 2, 3 \tag{1}$$

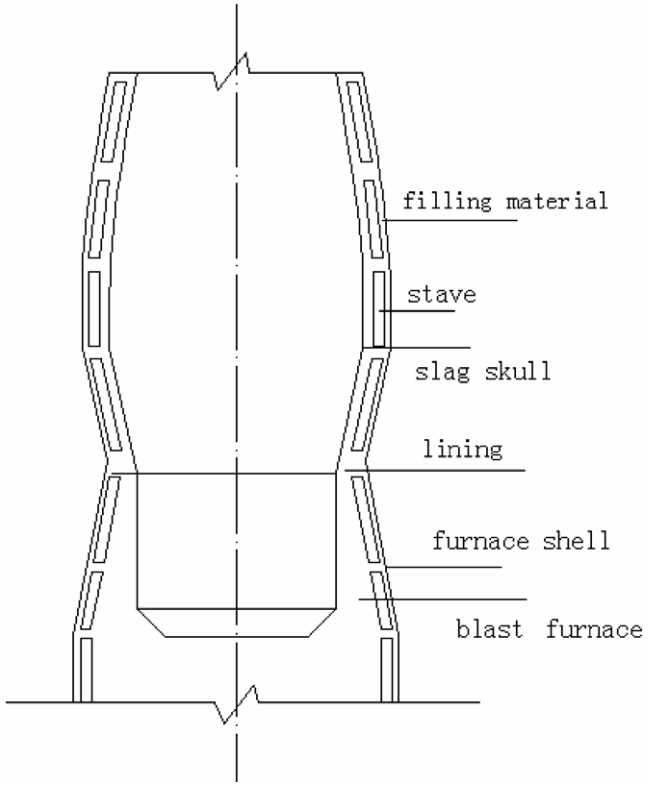

Fig. 1. Blast furnace and cooling stave.

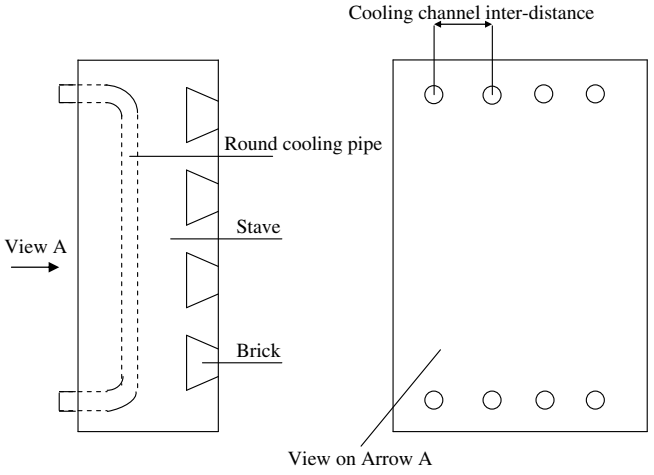

Fig. 2. Cooling stave.

Boundary conditions:

Between atmosphere and furnace shell

$$\lambda\frac{\partial T}{\partial x} = h_k(T_k - T_a) \tag{2}$$

Between slag skull and high temperature gas flow

$$\lambda\frac{\partial T}{\partial x} = h_z(T_g - T_z) \tag{3}$$

Between cooling stave and cooling water

$$\lambda\frac{\partial T}{\partial n} = h_{wb}(T_{wb} - T_{wa}) \tag{4}$$

$$\lambda\frac{\partial T}{\partial y} = 0 \quad y = 0, S \tag{5}$$

$$\lambda\frac{\partial T}{\partial z} = 0 \quad z = 0, H \tag{6}$$

2.1.1. Value of h_k

The overall coefficient of heat convection between furnace shell and atmosphere is given by

$$h_k = h_{k1} + h_{k2} \tag{7}$$

where h_{k1} is the coefficient of natural heat convection between furnace shell and atmosphere; h_{k2} is the radiative coefficient of heat convection between furnace shell and atmosphere, W/(m^2 °C).

For the calculation of h_{k1}, an equation can be described as follows according to the rule of natural heat convection:

$$Nu = c(Gr \cdot Pr)^n \tag{8}$$

Therefore, the value of h_{k1} is given as

$$h_{k1} = Nu\frac{\lambda_{air}}{l} = c(Gr \cdot \mathrm{Pr})^n\frac{\lambda_{air}}{l} \tag{9}$$

where l is the characteristic length of heat surface, namely the calculational high of the erect furnace shell [12], 1.385 m. On the surface of the erect cylinder, the Reynolds number is $Re = 8565$. It belongs to transitional flow and the Grash number $\mathrm{Gr} = 3.4 \times 10^9$. Hence, c, n is 0.0292 and 0.39, respectively according to Ref. [12].

The coefficient h_{k2} is given as

$$h_{k2} = \varepsilon C_0[(T_k + 273)^4 - (T_a + 273)^4]/(T_k - T_a) \tag{10}$$

where ε is the emissivity of furnace shell surface, 0.3; C_0 is the Planck constant, 5.67×10^{-8} W/(m^2 K^4).

2.1.2. Value of h_{wb}

The heat transfer between stave body and cooling water is shown in Fig. 4. The total heat resistance between cooling water and stave body contains the convection heat resistance between cooling water and water scale R_1; the conductive resistance of cooling water scale on the inner surface of cooling water pipes R_2; the conductive resistance of the steel pipe wall R_3; the heat resistance of the coating layer on the external surface of the cooling water pipe R_4 and the heat resistance of the gas clearance between the coating layer and the stave body R_5. Therefore, the overall coefficient of heat convection between the cooling stave and the cooling water h_{wb} is given by

$$h_{wb} = 1/R \tag{11}$$

where R is the total heat resistance between the cooling water and the stave body, (m^2 °C)/W, which can be described by the follows [5,8]:

$$R = R_1 + R_2 + R_3 + R_4 + R_5 \tag{12}$$

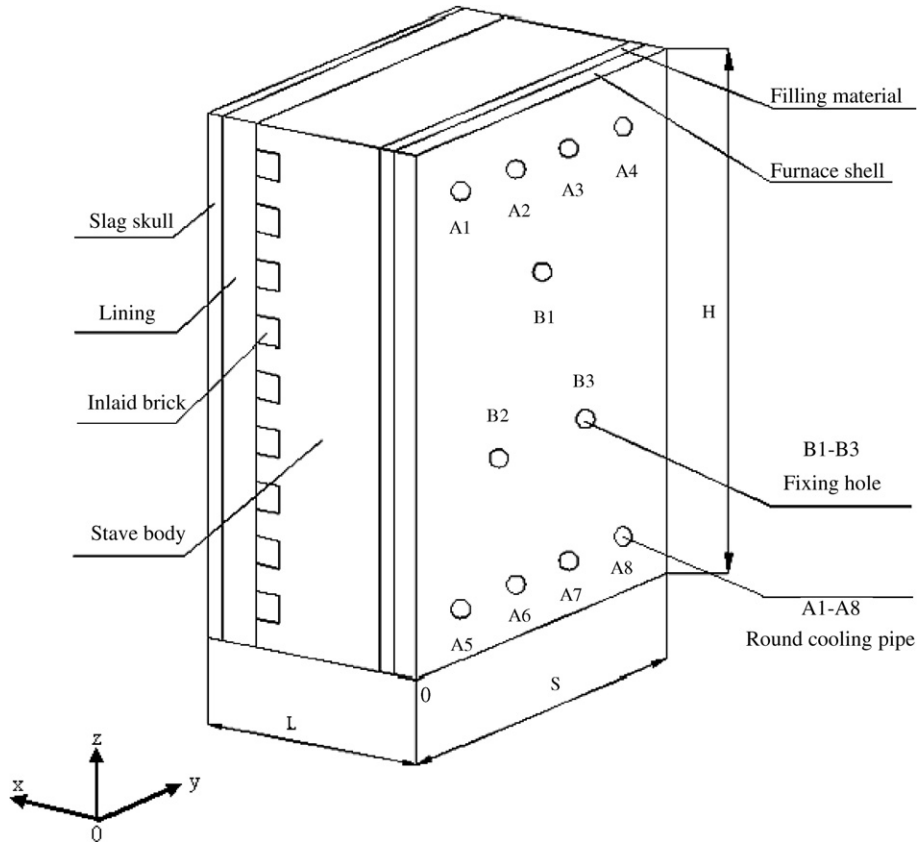

Fig. 3. Three-dimensional schematic of model.

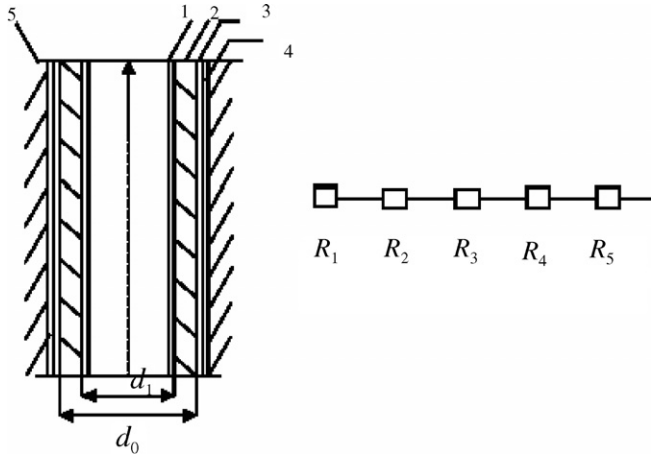

Fig. 4. Heat transfer between the stave body and the cooling water 1, water scale; 2, water pipe; 3, coating layer; 4, gas clearance; and 5, stave body.

2.1.2.1. Convection heat resistance between cooling water and water scale R_1. The convection heat resistance between cooling water and water scale R_1 is

$$R_1 = \left(\frac{1}{\alpha_w}\right)$$

Because of forced convection, the formula of Dittus-Boelter can be adopted as follows [12]:

$$Nu = \alpha_w d_1/\lambda_w = 0.023(vd_1/v)^{0.8}(v/\alpha_w)^{0.4} \quad (13)$$

$$\text{then} \quad \alpha_w = 0.023(v^{0.8}\lambda^{0.6}c_p^{0.4}\rho^{0.4})/(d_1^{0.2}v^{0.4}) \quad (14)$$

where v is the velocity of cooling water, m/s. When cooling water temperature is 30 °C, λ_w the thermal conductivity coefficient of cooling water is 0.618 W/(m^2 °C); c_p is the specific heat capacity of cooling water, 4.174 kJ/(kg K); ρ is the cooling water density, 995.6 kg/m^3; υ is the kinetic viscosity of cooling water, 0.805×10^{-6} m^2/s.

2.1.2.2. Conductive resistance of cooling water scale R_2. The conductive resistance of cooling water scale on the inner surface of cooling water pipes R_2 is

$$R_2 = \sigma_d/\lambda_d \quad (15)$$

where σ_d is the water scale thickness, 0.001 m; λ_d is the thermal conductivity coefficient of water scale, 1.7 W/(m °C).

2.1.2.3. Conductive resistance of the steel pipe wall R_3. The conductive resistance of the steel pipe wall R_3 is

$$R_3 = (d_0/2\lambda_p)\ln(d_0/d_1) \quad (16)$$

where λ_p is the thermal conductivity coefficient of steel pipe, W/(m °C); d_1 the inner diameter of the steel pipe, m; d_0 the external diameter of the steel pipe, m.

2.1.2.4. Heat resistance of the coating layer R_4. The heat resistance of the coating layer on the external surface of the cooling water pipe R_4 is

$$R_4 = \delta_c/\lambda_c \tag{17}$$

where δ_c is the thickness of coating layer on the external surface of the cooling water pipe, 0.0002 m; λ_c the thermal conductivity coefficient of coating layer, 0.8 W/(m °C).

2.1.2.5. Heat resistance of the gas clearance R_5. The gas clearance is formed during casting because of the temperature and thermal expansion coefficient difference between the cooling water pipe and stave body. The thickness of the gas clearance is about 0.1–0.3 mm. Because the gas clearance is very thin, it can be treated as a plane plate. According to thermal flux balance, an equation can be given as follows:

$$\frac{t_2 - t_c}{\frac{\delta_g}{\lambda_e}} = \frac{t_2 - t_c}{\frac{\delta_g}{\lambda_g}} + \frac{c_0(T_2^4 - T_c^4)}{\left(\frac{1}{\varepsilon_1} + \frac{1}{\varepsilon_c} - 1\right)}$$

where λ_e is the equivalent thermal conductivity of the gas clearance, W/(m °C); λ_g is the gas clearance thermal conductivity, 0.0385 W/(m °C); δ_g is the thickness of the gas clearance layer, m; ε_1 is the emissivity of stave body, 0.8; ε_c is the emissivity of coating layer, 0.8.

The heat resistance of the gas clearance can be determined as follows:

$$R_5 = \delta_g/\lambda_e = \frac{1}{\frac{1}{\frac{\delta_g}{\lambda_g}} + \frac{C_0(T_2^2+T_c^2)(T_2+T_c)}{\left(\frac{1}{\varepsilon_1}+\frac{1}{\varepsilon_c}-1\right)}}$$

So Eq. (11) can be modified as

$$\begin{aligned} h_{wb} &= 1/R \\ &= 1/[(1/\alpha) + \delta_d/\lambda_d + (d_0/2\lambda_w)\ln(d_0/d_1) + \delta_c/\lambda_c \\ &\quad + \delta_g/\lambda_e] \end{aligned} \tag{18}$$

2.1.3. Value of h_z

The value of h_z is made of the convection heat transfer between the gas flow and slag skull and the radiation heat transfer between solid materials (namely coke and ore) and slag skull.

Under the normal operation of a blast furnace, there is a slag skull adhering to the lining that protects the stave. Gudenau et al. [13] obtained convection coefficient between gas flow and slag skull (or lining) by the combination of the mathematical model of BF and in-site measurement. The convection coefficient is calculated when the gas flow temperature is 1200 °C, whose value shows 230 W/(m^2 °C).

The solid materials are convex and the area of solid materials is 0.8 times that of slag skull. The radiation heat transfer between solid materials and slag skull is given as follows [12]:

$$\varepsilon_s A_1 \times C_0[(T_{ko})^4 - (T_s)^4] = A_2 h_r (T_{ko} - T_s) \tag{19}$$

where

$$\varepsilon_s = \frac{1}{\frac{1}{\varepsilon_{ko}} + \frac{A_1}{A_2}\left(\frac{1}{\varepsilon_s} - 1\right)} \tag{20}$$

where ε_s is the emissivity of system, namely correct factor. A_1 is the area of solid materials, m^2; A_2 is the area of stave surface m^2; ε_{ko} is the emissivity of solid materials, 0.8; ε_s is the emissivity of stave surface, 0.8; T_{ko} is the temperature of solid materials, 1273 K; T_s is the temperature of slag skull surface, 773 K; h_r is the radiation heat transfer coefficient between solid materials and slag skull, W/(m^2 °C).

Formulas (19) and (20) show that $h_r = 142$ W/(m^2 °C). The overall convection coefficient between high temperature gas flow and solid materials and slag skull is $h_z = 230 + 142 = 372$ W/(m^2 °C).

2.2. Model of thermal stress field of steel cooling stave

Thermal stresses are a form of internal stressing arising from restricted thermal expansion or contraction of a body. Such restriction arises when a temperature gradient causes one part of a body to expand or contract more than another part. It also arises when a body which is not quite free to expand undergoes a change to the general level of its temperature [14]. It has been reported that the damage of the cooling stave and lining is mainly caused by the thermal stress change within the cooling stave and lining [2]. Therefore, understanding the thermal stress in the cooling stave and lining is essential for identifying conditions under which the cooling stave may be worn-out. The mathematical model of thermal stress of cooling stave will play an important role in the quantification of the thermal stress field in cooling stave and lining.

Some assumptions for calculation are as follows: (1) the thermal effects are in a steady state; (2) the energy arising from deforming is neglected; (3) the weight and external force of the cooling stave are neglected.

The compatible stress equations are given as follows [15]:

$$\nabla^2\sigma_x + \frac{1}{1+\mu}\frac{\partial^2\Theta}{\partial x^2} = -\alpha_t E\left(\frac{1}{1-\mu}\nabla^2 T + \frac{1}{1+\mu}\frac{\partial^2 T}{\partial x^2}\right)$$

$$\nabla^2\sigma_y + \frac{1}{1+\mu}\frac{\partial^2\Theta}{\partial y^2} = -\alpha_t E\left(\frac{1}{1-\mu}\nabla^2 T + \frac{1}{1+\mu}\frac{\partial^2 T}{\partial y^2}\right)$$

$$\nabla^2\sigma_z + \frac{1}{1+\mu}\frac{\partial^2\Theta}{\partial z^2} = -\alpha_t E\left(\frac{1}{1-\mu}\nabla^2 T + \frac{1}{1+\mu}\frac{\partial^2 T}{\partial z^2}\right)$$

$$\nabla^2\tau_{xy} + \frac{1}{1+\mu}\frac{\partial^2\Theta}{\partial x\partial y} = -\frac{\alpha_t E}{1+\mu}\frac{\partial^2 T}{\partial x\partial y}$$

$$\nabla^2\tau_{yz} + \frac{1}{1+\mu}\frac{\partial^2\Theta}{\partial y\partial z} = -\frac{\alpha_t E}{1+\mu}\frac{\partial^2 T}{\partial y\partial z}$$

$$\nabla^2\tau_{zx} + \frac{1}{1+\mu}\frac{\partial^2\Theta}{\partial z\partial x} = -\frac{\alpha_t E}{1+\mu}\frac{\partial^2 T}{\partial z\partial x}$$

where Θ is the bulk force and $\Theta = \sigma_x + \sigma_y + \sigma_z$.

Boundary conditions:

The bottom and top faces of the cooling stave are restricted, the other free.

Because the cooling stave is made of various materials, the behaviour of the contact interfaces between stave body and brick lining and between stave body and inlaid brick is considered. Here, the contact problem belongs to rigid-to-flexible contact problems, i.e. the stave body contact surface is treated as rigid, brick as flexible. ANSYS supports rigid-to-flexible surface-to-surface contact elements. This is a thermal-stress coupled-field problem where a thermal-stress analysis using the indirect method of ANSYS is made. The results from thermal analysis become loads for the stress analysis. The stress results are indicated by means of equivalent Von Mises thermal stress.

2.3. Comparison between calculated data and experimentized data

To demonstrate the validity and reliability of model of temperature field of the cooling stave, the stave temperatures estimated by heat transfer model were compared with the temperatures measured during thermal load test. The experimental furnace is shown in Fig. 5.

In this furnace, thermal loads corresponding to furnace temperatures between 500 and 1300 °C were applied using diesel oil as a fuel. The water velocity was 2.0 m/s. The stave was furnished with a large number of thermocouples in three measuring planes to be able to detect the planes' temperature behaviour. The evaluation of the temperatures always started after steady-state conditions were attained.

The results of comparison are shown in Fig. 6. It should be noted that the difference between the calculated value and the measured value is less than 20–30 °C. The degree of consistency is good. Accordingly, the stave temperature can be estimated with a considerably high accuracy using the values calculated by the heat transfer model.

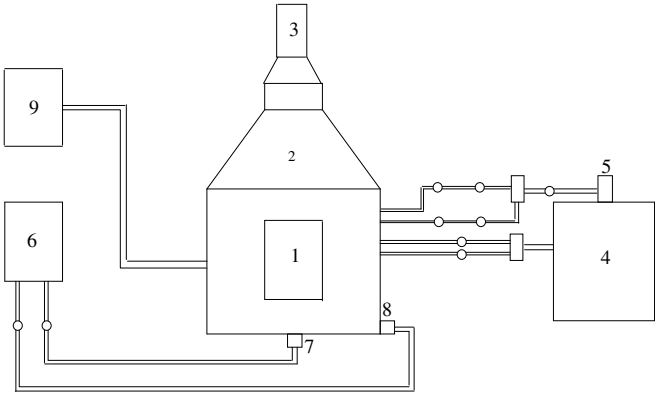

Fig. 5. Experimental rig of the cooling stave of BF 1, stave; 2, furnace; 3, chimney; 4, water tank; 5, pump; 6, oil tank; 7,8, burners; 9, operation platform.

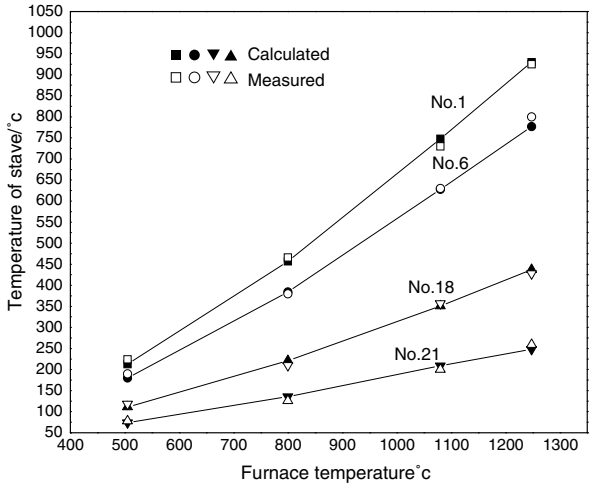

Fig. 6. Comparison of calculated value and measured value.

3. Results and effect of kinds of parameters on stave

The temperature and thermal stress fields of blast furnace stave are calculated by using the finite element software ANSYS. The thermal stress field has been calculated by the sequential method of coupled-field analysis. That is, the nodal temperatures from the thermal analysis are applied as "body force" loads in the subsequent stress analysis [16]. The size information and standard conditions of stave are listed in Table 1. The relevant parameters used in the computer simulation are listed in Tables 2 and 3.

The above-mentioned model is built for all the blast furnaces, with different material of cooling stave for different blast furnace. The model and results obtained can be applied to all the blast furnaces.

The gas flow temperature is assumed to be 1200 °C, the calculation results are as follows.

3.1. Effect of the cooling water velocity

The locations of the maximum temperature and stress are on the surface of the stave. The effect of the cooling water velocity (under the same cross sectional area) on the maximum temperature and thermal stress of the stave hot surface is shown in Fig. 7. It can be seen that the cool-

Table 1
The size information and standard conditions of stave (Unit, mm)

Stave length L	Stave width *S*	Stave high *H*	Furnace shell thickness
348	707	1385	10
Filling layer thickness	Stave body thickness	Inlaid brick thickness	Lining thickness
8	220	80	100
Slag layer thickness	Water pipe inner diameter	Water pipe external diameter	Cooling channel inter-distance
10	40	50	200

Table 2
Material parameters

Item	ρ (kg/m^3)	λ (W/m °C)	c_p (J/kg °C)
Furnace shell	7840	$52.2-0.025t$	465
Filling material	330	0.35	876
Cast steel	7800	$52.2-0.025t$	500
High alumina brick	2750	$2.09+0.000215t$	$808+0.314t$
Silicon carbide brick	2400	$21-0.009t$	$963+0.147t$
Silicon nitrogen bond silicon	2640	16.8	1000
Semi-graphite carbide brick	1700	$36.4-0.017t+6.389t^2$	1000
Graphite carbide brick	1700	13.5	840
Slag skull	2000	1.2	983
Water scale	2000	1.7	900
Coating layer	2000	0.8	900
Gas clearance	0.95	0.0385	1.068

t is the material temperature, °C.

Table 3
Material mechanical properties

	Temperature (°C)	Young's modulus (Pa)	Poisson's ratio	Coefficient of linear thermal expansion (1 °C^{-1})
Cast steel or furnace shell	30	2.06×10^{11}	0.3	1.06×10^{-5}
	500	1.70×10^{11}	0.3	1.06×10^{-5}
	1000	0.90×10^{11}	0.3	1.06×10^{-5}
	1500	0.20×10^{11}	0.3	1.06×10^{-5}
Silicon carbide brick	200	2.10×10^{10}	0.1	4.70×10^{-6}
	500	1.50×10^{10}	0.1	4.70×10^{-6}
	800	1.20×10^{10}	0.1	4.70×10^{-6}
	1370	0.70×10^{10}	0.1	4.70×10^{-6}
Filling material		2.10×10^{10}	0.1	4.70×10^{-6}
Slag skull		2.10×10^{10}	0.1	4.70×10^{-6}

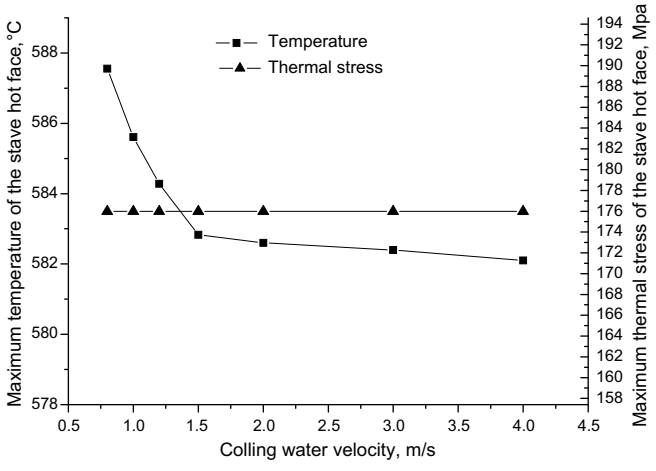

Fig. 7. Effect of the cooling water velocity on the maximum temperature and the thermal stress of the stave hot face.

ing water velocity has an influence on the maximum temperature of the stave hot surface but no influence on the thermal stress of the stave.

As we know, cooling water velocity is very important in avoiding film boiling. Film boiling occurs if the heat is supplied more quickly through the cast steel stave to water than it can be evacuated by bulk water. However, only increasing the cooling water velocity [17] is not very economical, because the maximum temperature of the stave hot surface decreases 4 °C when the water velocity changes from 0.8 to 4.0 m/s. The temperature of the stave hot surface presents no obvious improvement.

3.2. Effect of the cooling channel inter-distance

From Fig. 8, it can be observed that the cooling channel inter-distance has a large influence on the stave. Because the larger the cooling channel inter-distance, the few the number of the cooling channels which will induce the increase of the maximum temperature and thermal stress of the cooling stave.

3.3. Effect of the cooling channel diameter

Fig. 9 shows the effect of the cooling channel radius on maximum temperature and thermal stress of the stave body hot surface. The maximum temperature of the stave hot surface decreases, but the thermal stress increases with the increment of the cooling channel radius. The location of the maximum thermal stress does not lie on the stave hot surface, but on the interface between cooling water pipe and stave body. This is because the temperature gradient increases between cooling water pipe and stave body.

3.4. Effect of the lining material

The effect of different lining material on maximum temperature and thermal stress of the stave hot face is shown in Fig. 10. The value of maximum temperature and thermal stress of the stave hot surface is the highest when using the semi-graphite carbon brick lining, higher when using silicon nitrogen bond silicon carbide brick, graphite carbon brick or silicon carbide brick, and the lowest when using

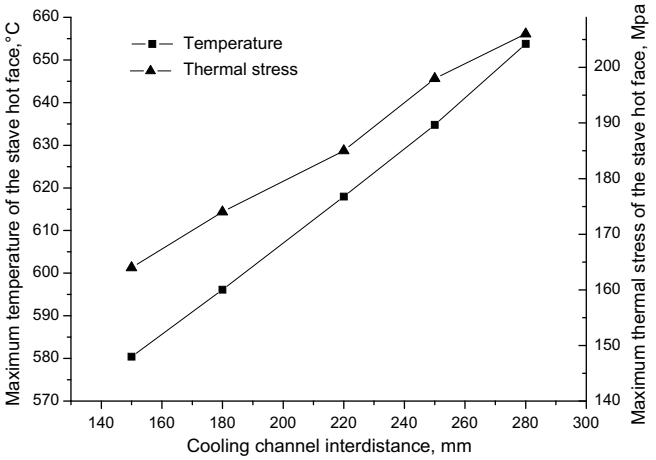

Fig. 8. Effect of the cooling channel inter-distance on the maximum temperature and the thermal stress of the stave hot face.

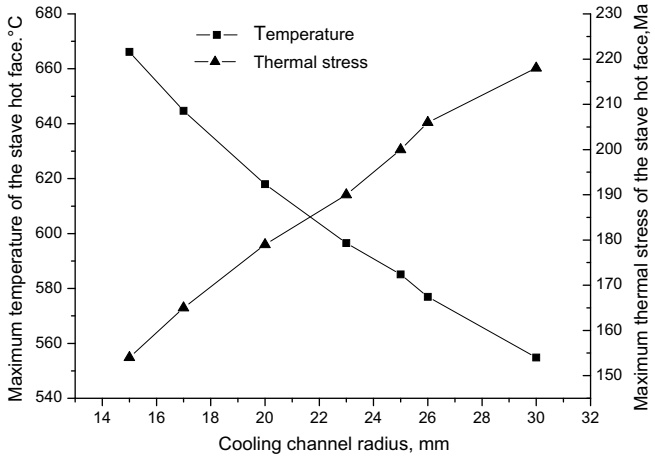

Fig. 9. Effect of the cooling channel radius on the maximum temperature and the thermal stress of the stave hot face.

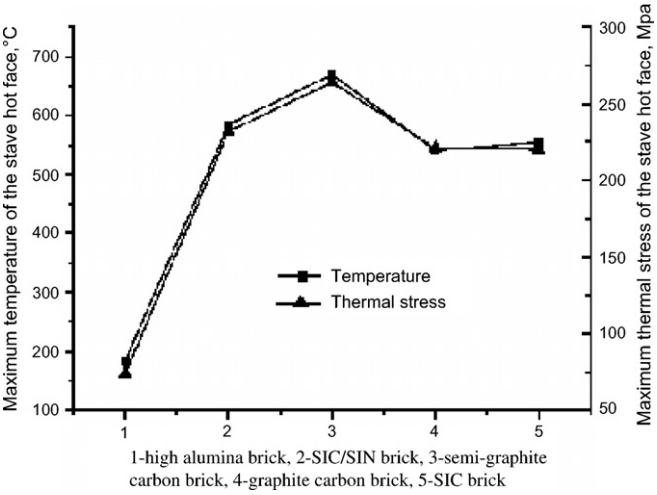

Fig. 10. Effect of different lining material on the maximum temperature and the thermal stress of the stave hot face.

high alumina brick. Compared with other refractory bricks, the high alumina brick is the lowest in flexural and compress strength, so it cannot withstand the adverse circumstances like scouring of the high temperature and the melting slag and iron; friction and impact of the blast furnace charge as well as the penetrating of the alkali metals.

Therefore, the suitable lining for stave is silicon nitrogen bond silicon carbide brick or silicon carbide brick.

3.5. Effect of the cooling water temperature

Fig. 11 shows the effect of cooling water temperature on maximum temperature and thermal stress of the stave hot surface. It can be seen that water temperature has a linear influence on the maximum temperature and thermal stress of the cooling stave. However, seeking for the lowest possible water temperature would be uneconomical. The water

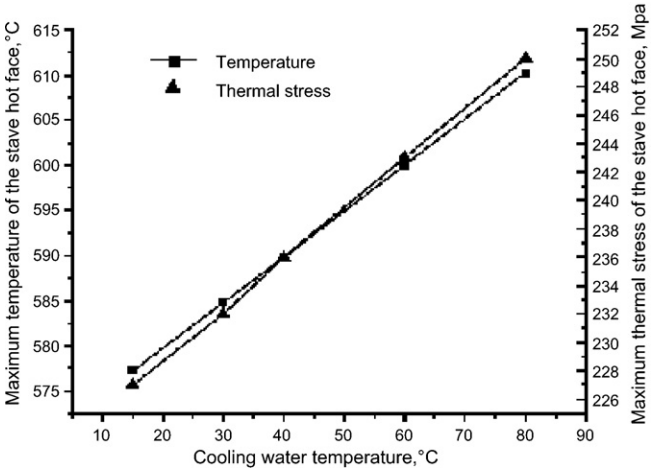

Fig. 11. Effect of cooling water temperature on the maximum temperature and the thermal stress of the stave hot face.

temperature can be chosen according to the local conditions, i.e. between 30 and 40 °C.

3.6. Effect of the cooling water scale

The water scale on the inner surface of the pipe is easy to be formed because of the reaction of electrochemical corrosion between water and inner surface of the pipe, and also there is a small quantity of sparry suspensions. The effect of the cooling water scale on the stave is shown in Fig. 12, which indicates the maximum temperature and thermal stress of the stave hot surface increase obviously increased with the increasing of the thickness of water scale. The maximum temperature will increase about 80 °C, thermal stress about 30 MPa when the thickness of water scale increase by 1 mm.

3.7. Effect of the coating layer on the external surface of the cooling water pipe

In order to avoid cooling water pipe being burned out while casting, the coating layer is coated on the external

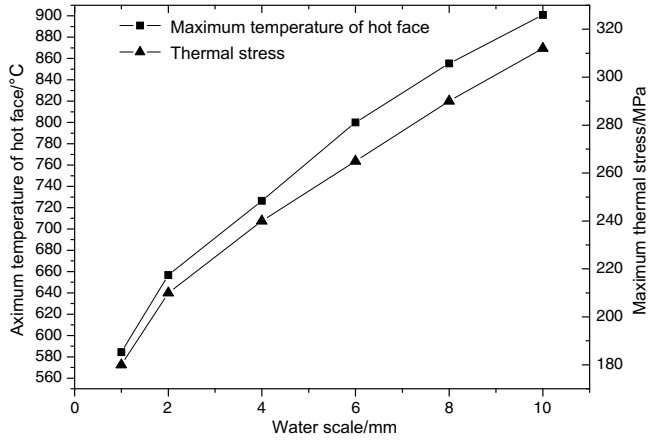

Fig. 12. Effect of the water scale on the maximum temperature and the thermal stress of the stave hot face.

surface of the pipe. The coat layer will decrease the cooling capacity of the stave. The effect of the coating layer on the external surface of the pipe is shown in Fig. 13, which indicates the maximum temperature of the stave hot surface is increased with the increasing of the thickness of the coating layer, but it is not distinct. The maximum temperature of the stave hot surface will increase about 3 °C with 0.1 mm increasing of the thickness of the coating layer. The maximum thermal stress of the stave hot surface does not change much with the variety of thickness of coat layer.

3.8. Effect of gas clearance

There is more or less gas clearance between the water pipe and the stave body while casting. The effect of the gas clearance on the maximum temperature and thermal stress of stave hot surface is shown in Fig. 14, which indicates the maximum temperature and thermal stress of the stave hot surface increase rapidly with the increasing of the thickness of gas clearance and the maximum temperature of stave hot surface will be more than 700 °C when the thickness of gas clearance is 0.2 mm. The maximum temperature of the stave hot surface will increase about 80 °C, the maximum thermal stress about 20 MPa when the gas clearance increases by 0.1 mm. Therefore, reducing the thickness of gas clearance is key to quality guarantee of stave.

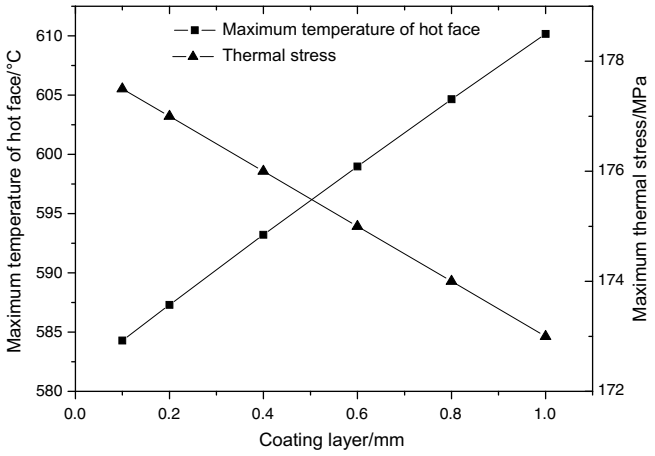

Fig. 13. Effect of the coating layer on the maximum temperature and the thermal stress of the stave hot face.

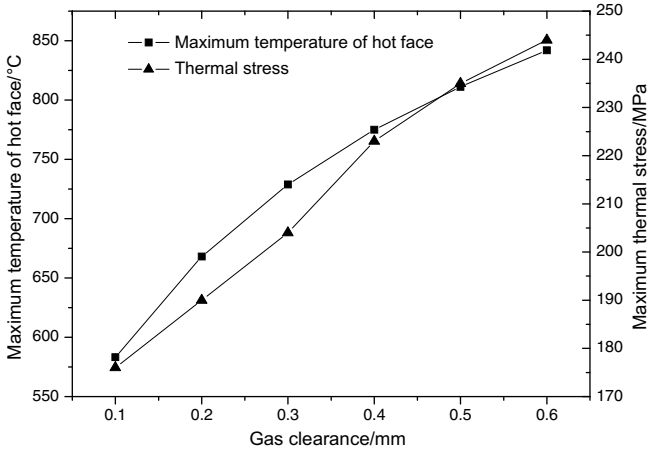

Fig. 14. Effect of the gas clearance on the maximum temperature and the thermal stress of the stave hot face.

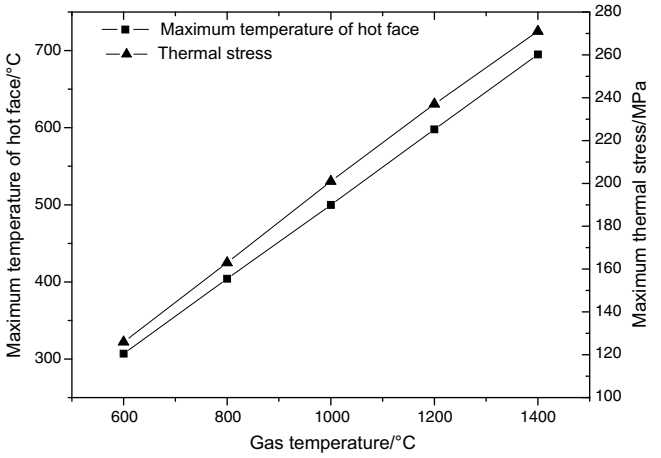

Fig. 15. Effect of the gas flow temperature on the maximum temperature and the thermal stress of the stave hot face.

3.9. Effect of gas flow

Fig. 15 shows the effect of the gas flow temperature on the maximum temperature and thermal stress of the stave hot surface. It can be seen that the gas flow temperature has a linear influence on the maximum temperature and thermal stress of the cooling stave. The maximum temperature is over 700 °C and the maximum thermal stress is nearly 300 MPa when the gas flow temperature is 1400 °C. The ductile stave will be faced with the danger of burning out. Therefore, steady blast furnace operation is the key to avoiding pipeline gas flow at the edge of the furnace wall.

4. Conclusions

In this paper, the three-dimensional mathematical model of temperature and thermal stress fields of blast furnace stave and lining has been built under the assumption that the system is in the steady state. Particularly, the radiation heat transmission from solid materials (coke and ore) to the inner surface of the stave is taken into account, which has so far been neglected by other researchers. The finite element soft ANSYS is used to calculate the model and the experiment results are used to validate the numerical calculations. Heat transfer analysis is made of the effect of the cooling water velocity and temperature, the gas flow temperature, the cooling channel inter-distance and diameter, the inlaid brick thickness, the stave body thickness, the

lining material, the cooling water scale, the coating layer on the external surface of the cooling water pipe as well as the gas clearance on the maximum temperature and thermal stress of hot surface of the stave was analyzed by heat transfer analysis. The results of the calculations show that reducing the water temperature and increasing the water velocity would be uneconomical. The primary reason of stave dilapidation is the formation of the pipeline high temperature gas flow at the edge of blast furnace wall. As a consequence, the heat transfer and hence the maximum temperature and thermal stress in the stave can be controlled by properly adjusting the operating conditions of the blast furnace, such as the gas flow, the cooling channel inter-distance and diameter, the lining material, the coating layer and the gas clearance.

References

[1] Robert W. Steiger, Robert E. Braun, David P. Grundtisch, Utilization of computer analysis in blast furnace refractory lining and shell design, Ironmaking Conf. Proc. 44 (1985) 485–504.
[2] G.X. Wang, A.B. Yu, P. Zulli, Three-dimensional modelling of the wall heat transfer in the lower stack region of a blast furnace, ISIJ Int. 37 (5) (1997) 441–448.
[3] S. Chen, Y. He, Q. Wu, Temperature field computation of stave in blast furnace operation, Iron Steel (Peking) 29 (1) (1994) 52–56 (in Chinese).
[4] M. Wu, L. Wang, S. Liu, Three-dimensional heat transfer model for stave and lining of blast furnace, Iron Steel (Peking) 30 (3) (1995) 6–11 (in Chinese).
[5] Y. Song, T. Yang, M. Wu, S. Liu, Calculation and analysis on cooling capacity of blast furnace stave, Iron Steel (Peking) 31 (10) (1996) 9–13 (in Chinese).
[6] S. Chen, Q. Xue, D. Cang, T. Yang, Heat transfer analysis of blast furnace stave, Iron Steel (Peking) 34 (5) (1999) 11–13 (in Chinese).
[7] S. Chen, T. Yang, W. Yang, Q. Quan, Q. Wu, Analysis of heat transfer and temperature field of blast furnace copper stave, Iron Steel (Peking) 36 (2) (2001) 8–11 (in Chinese).
[8] S. Chen, Q. Xue, W. Yang, M. Wu, T. Yang, Designing for long campaign life blast furnace(1) – the mathematical model of temperature field for blast furnace lining and cooling apparatus and new concept of long campaignship blast furnace cooler design, J. Univ. Sci. Tech. Beijing 6 (3) (1999) 178–182.
[9] Q. Xue, W. Yang, S. Chen, M. Wu, T. Yang, Designing for long campaign life blast furnace(2) – the simulation of temperature field of lining and cooling apparatus, J. Univ. Sci. Tech. Beijing 7 (1) (2000) 30–33.
[10] Wu Lijun, Zhou Weiguo, Cheng Huier, et al., The study of cooling channel optimization in blast furnace cast steel stavebased on heat transfer analysis, Int. J. Adv. Manufac. Tech. 29 (1–2) (2006) 64–69.
[11] Qian Zhong, Du Zhaohui, Wu Lijun, Transient heat transfer analysis of blast furnace cooling staves, Steel Res. Int. 78 (1) (2007) 19–23.
[12] Yang Shiming, Tao. Wenquan, Heat Transfer, Higher Education Publishing Company, Beijing, 2001 (in Chinese).
[13] Heinrich Wilhelm Gudenau, Nikolas Standish, Wolfram Gerlach, Die physikalischen Verhältnisse im Bereich der kohäsiven Zone des Hochofens(Teil 1: Grundlagen und Modelle), Stahl u. Eisen 112 (8) (1992) 73–79.
[14] P.P. Benham, Russell Hoyle, Thermal Stress, Sir Isaac Pitman & Sons Ltd., 1964.
[15] Z. Gu, Y. Ge, Z. Weng, X. Ye, J. Yang, Engineering Thermal Stress, National Defence Industry Publishing Company Beijing, Beijing, 1987 (in Chinese).
[16] Zhang Shengming, Structure Analysis Based on ANSYS, Qing Hua University Company, Beijing, 2003 (in Chinese).
[17] R. Thill, A. Poensgen, I. Carmichael, Paul Wurth, S.A. Luxembourg, The application of FEM techniques in the development of copper stave for the high heat load and hearth areas of the blast furnace, Ironmaking Conf. Proc. (2000) 155–166.